AD-A071 760 WASHINGTON UNIV SEATTLE DEPT OF ATMOSPHERIC SCIENCES F/G 4/1
A STUDY OF THE SPATIAL AND TEMPORAL VARIATION OF TEMPERATURE IN--ETC(U)
JUN 79 J E TILLMAN DAHC04-74-G-0022

UNCLASSIFIED ARO-11586.1-EN NL

| OF |
AD
A071760

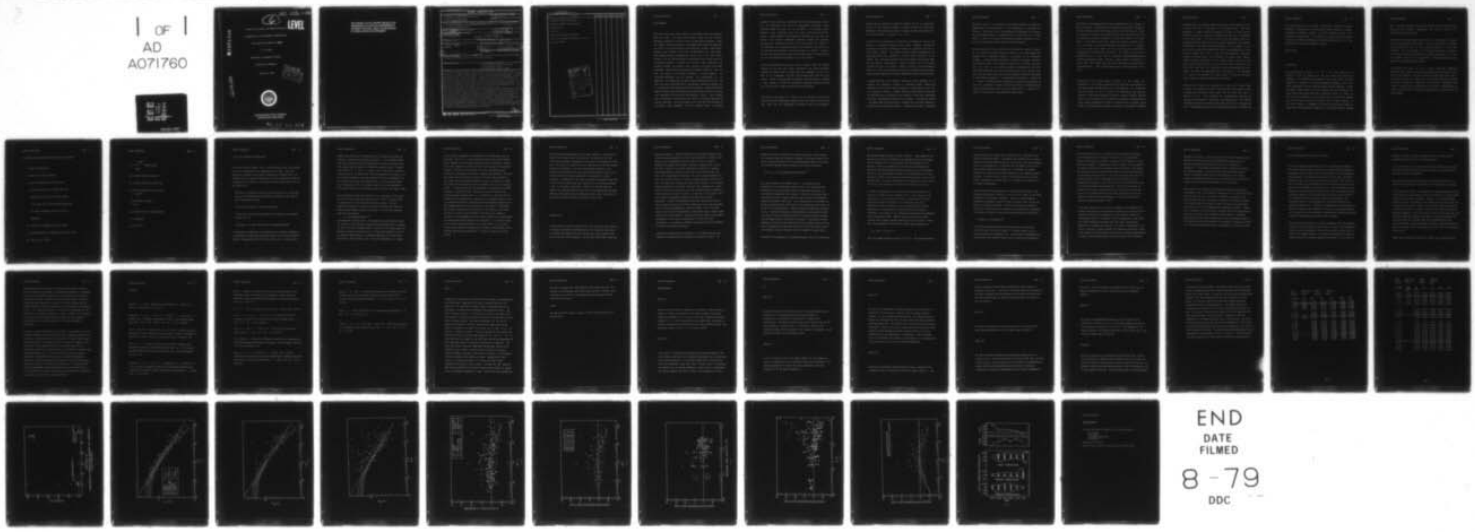

END
DATE
FILMED
8-79
DDC

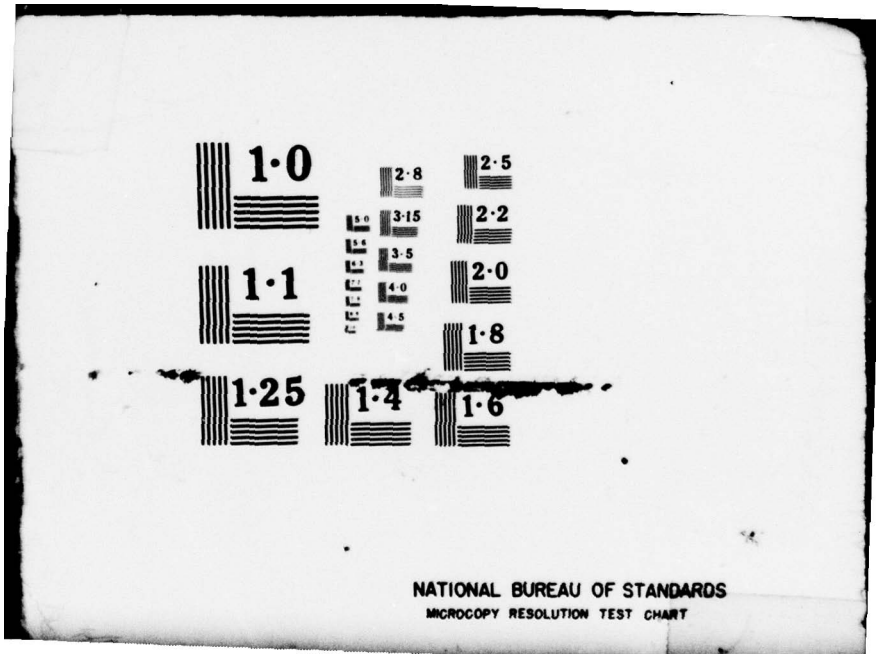
1·0
1·1
1·25
2·8
3·15
3·5
4·0
4·5
5·0
2·5
2·2
2·0
1·8
1·4
1·6
NATIONAL BUREAU OF STANDARDS
MICROCOPY RESOLUTION TEST CHART

A Study of the Spatial and Temporal Variation of Temperature in the Atmospheric Boundary Layer

Final Report Grant DAHC04 74 G0022

J. E. Tillman

Department of Atmospheric Sciences

University of Washington

Seattle Wa. 98195

THE FINDINGS IN THIS REPORT ARE NOT TO BE CONSTRUED AS AN OFFICIAL DEPARTMENT OF THE ARMY POSITION, UNLESS SO DESIGNATED BY OTHER AUTHORIZED DOCUMENTS.

Unclassified

Security Classification

DOCUMENT CONTROL DATA - R & D

(Security classification of title, body of abstract and indexing annotation must be entered when the overall report is classified)

1. ORIGINATING ACTIVITY (Corporate author)
Atmospheric Sciences Department AK-40
University of Washington
Seattle, Washington 98195

2a. REPORT SECURITY CLASSIFICATION
Unclassified

2b. GROUP
NA

3. REPORT TITLE
A Study of the Spatial and Temporal Variation of Temperature in the Atmospheric Boundary Layer

4. DESCRIPTIVE NOTES (Type of report and inclusive dates)
Final Report

5. AUTHOR(S) (First name, middle initial, last name)
James E. Tillman

6. REPORT DATE
June 15, 1979

7a. TOTAL NO. OF PAGES
48

7b. NO. OF REFS
14

8a. CONTRACT OR GRANT NO.
DAHC04 74 G0022

b. PROJECT NO.

c.

d.

9a. ORIGINATOR'S REPORT NUMBER(S)
ARO 11586.1-EV

9b. OTHER REPORT NO(S) (Any other numbers that may be assigned this report)

10. DISTRIBUTION STATEMENT
Approved for public release; distribution unlimited

11. SUPPLEMENTARY NOTES

12. SPONSORING MILITARY ACTIVITY
U.S. Army Research Office-Durham
Box CM, Duke Station
Durham, North Carolina 27706

13. ABSTRACT The ratio of σ_T/T_* for mixed and free convection has been examined as a function of heat flux, of the % of inversion height, and of the effects of water vapor on buoyancy. For the stability range $-Z/L>0.1$, the free convection similarity relation $\sigma_T/T_*=-0.95(-Z/L)^{-1/3}$ is accurate up to at least 60% of the inversion height. For the lower heights where forced convection is important the relation: $\sigma_T/T_*=-0.95(0.0549-Z/L)^{-1/3}$ provides a stability dependent correction for the heat flux. The effect of water vapor on the buoyant processes can be incorporated by substituting virtual temperature for temperature in the relations above. These relations also determine implicitly the buoyancy flux at the surface. This is a good approximation of the sensible heat flux as long as the Bowen ratio is larger than one.

The horizontal uniformity of minimum temperature during quiescent intervals for unstabl convection is shown to be on the order of a few hundreds of a degree celsuis over a fifty meter array for periods on the order of fifteen minutes. One interpretation of this characteristic is that the minimum temperature during the quiescent interval is characteristic of the potential temperature at planetary boundary layer heights at which the potential temperature is constant with height. Examination of the quiescent temperature during unstable and stable periods of the same day, shows that the spatially uniform quiescent temperatures go from cold during unstable conditions to war during stable conditions. The latter is consistent with the hypothesis that elements from height ranges of uniform potential temperature are advected into the surface layer by mechanical mixing during these stable conditions.

370 270

DD FORM 1 NOV 68 1473 REPLACES DD FORM 1473, 1 JAN 64, WHICH IS OBSOLETE FOR ARMY USE.

Unclassified

Security Classification

14. KEY WORDS	LINK A		LINK B		LINK C	
	ROLE	WT	ROLE	WT	ROLE	WT
temperature similarity theory						
unstable planteary boundary layer						
buoyancy flux						
heat flux						
quiescent temperature intervals						
spatial and temporal temperature statistics						
free convection						

FIELD PROGRAMS

Three sets of data were either partially or completely acquired and analyzed under this grant. The major field program funded was the Minnesoto experiment, conducted in the fall of 1973 in northwestern Minnesoto. (Izumi and Caughey, 1976) The University of Washington group joined the experiment as a guest of the United States Air Force Cambridge Research Laboratories' Boundary Layer Research Group, under the leadership of Dr. Duane Haugen. This cooperative mode of experiment was chosen due to the small budget required for the field progam and the anticipation that a major portion of the analysis required to provide the parameters that characterize the planetary surface and boundary layer would be a by product of the AFCRL experiment. Another reason for utilizing the AFCRL facilities is that the site was chosen for horizontal uniformity. In many respects, the anticipated advantages were not realized. Our participation in the experiment was delayed until the other groups had obtained their data. The AFCRL group lost two balloons due to meteorological phenomena, causing them to terminate the field program earlier than expected. The anticipated data analysis benefits were not realized as the efforts were devoted to the major joint experiment with the British Meteorological Office. Since problems were anticipated, we obtained real time output of 15 minute average profile and flux quantities. Due to the scatter of the real time field estimates of the boundary layer parameters from the measured fluxes, we obtained

estimates from the profiles of temperature and wind by analyzing the profile wind and temperature data using the flux-gradient relations. These quantities became the basis for our estimates of the boundary layer parameters after eliminating data from levels on the tower with faulty sensors. An added benefit of the program was obtaining the data from the balloon which provided temperature statistics throught the planetary boundary layer. Measuring the height of the inversion and it's effect on the parameters was an important factor in the experiment since this is our only data set over land where the inversion height is available. However, the data from this experiment taken at the heigher levels is anomolous which led to a more thorough investigation of the $\sigma_T/T_\star$ relation.

The site characteristics were not as ideal as expected since the extreme flatness of the area made slight indentations form muddy areas which remained an anomolous source of water vapor flux surrounded by dry soil. This may be responsible for some of the puzzling results from one or two sensors. However, the uniformity in roughness, with proper fetch, provided a good setting to verify the uniformity of potential temperature during quiescent intervals between the bouyant convective elements.

The puzzling $\sigma_T/T_\star$ versus Z/L relation for the Minnesoto balloon data warranted furthur investigation especially since this relation is one of the most stable and site independent encountered prior to this experiment.

Since the data in question was obtained at heights that are an appreciable fraction of the inversion height, as opposed to that of the tower based experiments data covering the range of planetary boundary layer heights was obtained and analyzed. (Hiester, T. R., 1977)

An objective of the program was to determine to what degree of accuracy the quiescent temperatures observed during highly unstable temperatures represented the potential temperature observed at a significant fraction of the inversion height. The Buffalo aircraft of NCAR was scheduled to fly during our phase of the experiment to permit direct comparison of the surface layer quiescent temperature with that measured over time and space from the aircraft. Unfortunately, structual problems with the aircraft cancelled this part of the program. However, the space and time variability within the array has been used to support the hypothesis that the parcels with quiescent temperatures originate significantly above the surface layer.

A primary objective of the Minnesota temperature array analysis was to determine the translation velocity of convective plumes. Ideally, the direction of the wind at the time of passage of a plume should be used for the translation velocity. However, because the time series of wind speed and direction were not available, it was necessary to make some assumptions concerning the translation direction of the plumes. As reported previously (our and/or other notes and papers), assuming that the plumes translate in the direction of the mean wind leads to substantially greater translation

velocities than if it is assumed that the plumes translate in a direction perpendicular to their orientation. (Their orientation is determined by fitting a plane wave to the sharp temperature discontinuity at the upwind edge using three sensors in a triangular array.) Since there is no clear reason to select one method of determining translation direction over the other, the translation velocity results remain inconclusive.

The second objective of the analysis was to determine the planform pattern of the plumes in a horizontal plane. However, to do so again requires the knowlege of the translation direction, in addition to the translation velocity. It was therefore impossible to determine the planform pattern of the convective plumes. The inconclusive results led to a second experiment which took place at the Boulder Atmospheric Observatory in April 1978. During this experiment, both wind speed and direction were measured along with the array temperature using the same temperature system as constructed for the Minnesota experiment. The measurements were made by J. Tillman and J. Wilczak. Preliminary results indicate that conclusive determination of both the translation velocity and planform structure of convective plumes will be possible from the data set and the results will be reported in a Master of Science thesis being prepared by James Wilczak.

The layout of the temperature sensor array constructed for this program is given in Figure 1. The majority of the sensors were located at a height of four meters along a south to north and a west to east line from the center of the array. The center was located 50 meters east of the AFCRL tower and our sensors were located at heights of 2,4,8,16 and 32 meters on the AFCRL tower. At the center of the array, sensors were located at heights of 0.5, 1. 2, and 4 meters. The vertical supporting poles were 7.5 cm in diamater and the sensors were located one meter from the poles to minimize the interception of hot plumes from the poles. The sensors are 25 micron platinum wire in a three wire AC synchronous modulation-demodulation resistance thermometer system. The basic system exhibits stabilities of better than 0.01 degrees over long periods exclusive of any stretching of the platinum wire. A more complete description is given by Katsaros, et al. 1977.

Calibration of the complete system, exclusive of the sensors was accomplished in the field by substituting five precision fixed resistors in each channel after the completion of the field experiment. The calibration data was written on tape in exactly the same manner as the data were collected. Sensors were calibrated to within a range of 3 degrees absolute using a bath of mineral oil and a calibration adjustment was made using the quartz crystal thermometers of AFCRL as a reference over a 15 minute period during the field program to improve the accuracy. The adjustment consisted

of assuming that the electronic system was accurate ot 0.01 degrees and that any errors were due to stretching of the platinum wire. With this assumption, a single parameter adjustment was made to bring the mean temperature of all array sensors into agreement with the quartz thermometer at the same height. The data of Table 1 show the reduction after this adjustment where the AFCRL and UW 15 minute mean temperatures are equivalent by definition. Note that the standard deviations of the sensors in the array agree to within 0.045 degrees even though the calibration was a single parameter change rather than a bias and a gain adjustment. Subsequent checks of the sensors, after the elimination of several noisy sensors, produced maximum differences of 0.12 degrees between any of the array sensors and the quartz sensors on the tower except below 2 meters where the AFCRL tower base and it's surrounding area are unrepresentative of the surface. Generally, the differences were on the order of a few hundredths of a degree. The subsequent run, shown in Table 2, 2 hours and 12 minutes later, indicates a maximum difference of 0.05 degrees.

Filtering of the signal was accomplished by three pole filters whose response was down by 50% at 10 Hz. The phase shift was controlled so that no signal channel differed in phase shift from any other more than 10 degrees at 10 Hz. Data collection was accomplished by a Raytheon 704 computer writing standard 7 track tapes. Data sampling rates were program selectable and there was no limit on the length of each run. Monitoring was done in background during real-time foreground digitizing at a maximum rate

of 50 samples per second per channel. Monitoring consisted of dumping functions of various sensors to strip charts, numeric display or a printer. The functions generally consisted of scaled temperature values or of differences between sensors. The selection of display functions and sensor selection was completely independent of foreground digitizing and is best categorized as a background algebraic language.

DATA ANALYSIS

Introduction

In an earlier paper (Tillman, J. E., 1972) the σ_T/T_* relation as a function of Z/L was examined with the aid of data from several field experiments. The formulation was extended to cover both forced and free convection as opposed to the prior formulations (Wyngaard, et al. 1971) which incorporated only free convection during unstable conditions. Another limitation of these results is that they include only "dry convection", i.e. those cases in which water vapor has no significant effect on either the heat flux or the stability. In the present paper, the results are extended to cover those cases in which the latent heat flux is a major component of the total surface to atmosphere heat flux and in which water vapor is a major factor in determining the buoyancy of the unstable planetary boundary

layer. The final limitation of the prior efforts is that the height of the inversion was not measured. Consequently, the effect of Z/Z_i on the formulation could not be tested.

Associated with the more complete results for the σ_T/T_* versus Z/L relation are the surface buoyancy flux results. With the new data sets, the effects of water vapor and of Z/Z_i on the calculated buoyancy flux have been estimated. From this analysis, it is clear that the surface to atmosphere total buoyancy flux can be estimated by the simple measurement of the mean and standard deviation of the appropriate temperature throught a major portion of the planetary boundary layer.

The uniformity over space and time of several temperature temperature statistics were analyzed using the array sensors during the period of from 1500 to 1700 on 9/28/79. This was a period with steady light winds from a favorable direction and during which the quiescent temperature intervals were common. Although no comaprisons with equivalent measurements from sensors located above the surface layer can be made, the observations over time and space are used to infrer some characteristics of these parcels and their origins.

The definitions and symbols for this paper are as follows:

Z = height of observation

Z_i = height of the first inversion

T = average temperature over time or space.

When latent heat flux << sensible heat flux, temperature is used in all statistics while in all other cases, (unless otherwise specified) the virtual temperature is used in place of temperature.

T' = deviation of temperature from the average

σ_T = standard deviation of temperature over time or space

$T_* = -H_0/\rho\ c_p u_* = -\overline{w'T'}/u_*$

$$L = - \frac{\rho c_p T u_*^3}{kgZH_0}$$ Obukhov length

Z/L = Obukhov stability parameter

H_0 = Surface-atmospheric buoyancy flux

H_Z = Vertical buoyancy flux at height Z

$= \rho c_p \overline{w'T'}$

k = von Karman's constant

= 0.35

c_p = specific heat at constant pressure

ρ = air density

$u_* = (-\overline{u'w'})^{1/2}$

σ_T/T_* in the Planetary Boundary Layer

In the prior work of Tillman (1972), several factors in the σ_T/T_* relation could not be investigated due to limitations of the data. Since this relation is the basis of the indirect computation of buoyancy flux, it is desirable that it's range of application be as wide as possible and that its limitations be well defined. The factors that were either poorly or not at all defined were:

The need for a stability correction for small values of Z/L where both buoyant and mechanically driven turbulence contribute to the fluxes of heat, momentum and moisture.

The effect of moisture on the buoyant processes.

The effect of the height of observation as a function of the inversion height, Z/Z_i, and

The effect of the actual heat flux on the measurement errors.

To understand the importance of the parameters not previously considered, it is appropriate to start with the relation between σ_T/T_* and Z/L as shown in Figure 2, incorporating both the old and new data sets. (Note that the

height range $0.0<Z/Z_i<0.8$ is presented while the complete layer below the inversion $0.0<Z/Z_i<1.0$ is presented in figure 3.) For the AMTEX, BOMEX, GATE , Great Lakes and Puerto Rico experiments, the data were obtained from flights using National Center for Atmospheric Research Aircraft (Hiester, 1977, Pennell, W. T. and M. A. LeMone. 1974. These data are hereafter referred to as "W" to indicate that they were obtained over the water.) For the Minnesota experiment, data were obtained from tower instrumentation up to 32 meters and from balloon instrumentation up to the inversion height (Izumi and Caughey, 1976). The Kansas, Round Hill and Utah experiments, KRU, provided the data for the earlier results (Tillman, 1972, Monji, 1972)

Several important factors are evident upon close inspection of this figure. The first is that the KRU data closely follow a $(Z/L)^{-1/3}$ relation which is characteristic of free convection similarity scaling. The only significant deviation is at the small values of Z/L where both forced and free convection control turbulent interchange. It is for this stability region that the function:

$$1)\quad \sigma_T/T_* = -0.95(0.0549-Z/L)^{-1/3}$$

was formulated (Tillman, 1972). The Minnesota data were added to verify the relation over the stability range previously encountered and to increase the data in the highly unstable region. Since this is the region where free convection similarity scaling and the -1/3 power law dependence of σ_T/T_* on Z/L should be most accurate, it is somewhat surprising to find the large deviations at the high values of Z/L. The first explanation is to assume

that the balloon measurments are responsible for the deviations, where in many cases, $Z/Z_i >> 0.1$. As the convective elements loose their buoyancy excess compared to the surrounding environment due to entrainment, inertial forces become dominant and "free convective" scaling might not be expected to apply. Partially for this reason, the W data, covering the range $0.0<Z/Z_i<1.0$, were added to this set for analysis and comparison. Note that even though the W data plotted in Figure 2 cover the range $0.0<Z/Z_i<0.8$, they scatter rather uniformly around the -1/3 power law relation for large -Z/L rather than falling below the free convection line as do the Minnesota values. To further explore the Z/Z_i dependence, the same data are plotted in Figure 3, stratified by Z/Z_i, except that the points now cover the complete planetary boundary layer, i.e., $0.0<Z/Z_i<1.0$. Note that with the exception of the Minnesota data, seven points in the range $0.8<Z/Z_i<1.0$, and a few surface based points, the majority of the planetary boundary layer is well characterized by the "free convection" σ_T/T_* relation. Consequently, one is led to conclude that the deviations of the Minnesota data at high values of Z/L from the "free convection" relation can not readily be attributed to Z/Z_i dependence and that they are probably due to instrumental or meteorological factors unique to this experiment. It is fortunate that the -1/3 power law relation holds to such large values of Z/Z_i, as this allows surface buoyancy flux determination throught a major portion of the boundary layer with great simplicity. This will be covered in the next section.

Data from aircraft measurements over the water, (Figure 4), illustrate the effect of water vapor on the σ_T/T_* relation. The scatter of the 'dry' calculation indicates the importance of water vapor in the majority of these data. (The error is so large for the dry assumption that some points exceed the upper plot boundary.) That the other experients produce a σ_T/T_* relation with low scatter when water vapor has been ignored, must be due to the small differences between statistics of temperature and virtual temperature. Examination of data from the Australian experiment (Shaw 1978) at a site with a stubble grass cover indicates that the difference between σ_T and σ_{TV} is at most a few percent. However, at many land sites and seasons, the latent/sensible heat flux ratio is much greater than one (Munn, 1966) and would thereby produce significant errors in any σ_T/T_* versus Z/L plots derived without including the effects of water vapor.

Buoyancy Flux

A major practical reason for exploring the σ_T/T_* relation in great detail is to evaluate the possible simplifications and the limitations when using it to determine the buoyancy flux in the general case and the sensible heat flux in the case of dry convection. For the tower based surface layer data

previously analyzed, a stability correction for the stability range Z/L<0.2 provided increased accuracy in the heat flux calculations. (Tillman, 1972) However, this is undesirable in that the heat flux can no longer be determined exclusively from constants, pressure, temperature and σ_T alone and either a direct or an indirect measurement of stability is required. Direct measurement of stability is difficult in that both heat flux and shear stress measurements are required. The shear stress measurements are noisy, even near the surface, in that for averaging periods of less than an hour, the values often fluctuate by several tens of percent. As one departs from the proximity of the surface, the scale sizes responsible for a major portion of the stress grow larger and longer averaging times are required to obtain estimates with similar accuracy. In addition to this problem, there are a number of instrumental problems associated with the stress measurement. Indirect determinations can be made using relations such as those relating the profiles of wind and temperature to the fluxes (Businger, 1973) or such as the skewness-Z/L relation (Tillman, 1972). The former require several levels of measurements, although they seem to produce stable estimates over smooth terrain. The latter may be as variable as the direct measurements, but the data are insufficient to verify this point. Consequently, it is valuable to determine the accuracy that can be obtained by ignoring the stability correction.

Examining the complete data set of Figure 2, it is evident that the free convective -1/3 power law fits fairly well for values of -Z/L>0.1. To

determine the effect of ignoring the stability correction, first consider the comparison using this correction, important for the small values of Z/L. Figure 5 presents the ratio of the calculated/measured buoyancy flux, where the calculated complete unstable buoyancy flux relation is given by:

$$2)\ H/\rho\ c_p = [(\sigma_T/C_1)^3(kgZ/T)(C2-Z/L)/(-Z/L)]^{1/2}$$

(For this calculation, the Obukhov length, L, is obtained from the measurement of it's constituient variables while in the earlier work by Tillman (1972), it was obtained solely from temperature statistics, i.e. the skewness of temperature- Z/L relation.) Note that the buoyancy flux is determined through the complete stability range and most of the planetary boundary layer without major bias. If the Minnesota data are excluded, the results are even better and the majority of the calculations fall within -25 to +30 % of the measured value. Figure 6 presents the same data stratified by Z/Z_i. The results indicate an underestimation of the buoyancy flux for high values of Z/L if the Minnesota data are included whereas the relation does not appear biased if these data are excluded. There may be an actual deviation from the free convection relation for the higher values of Z/L but these are generally also the cases where $Z/Z_i >> 0.1$ and the inertial forces are beginning to play an important role when compared to buoyant forces.

The effect of the magnitude of the measured buoyancy flux on the accuracy of

the complete unstable relation is shown in Figure 7. There appears to be a tendency for the error to decrease as the magnitude of the flux increases; this is especially true if the Minnesota data are eliminated from the analysis. This is not surprising in that the errors in measuring the temperature, and the buoyancy flux, should increase as the flux decreases. The plot of the σ_T/T_* relation of Figure 4 also illustrates the fact that ignoring the effect of water vapor can produce major errors in the heat flux determinations. The errors assuming only "dry" convection are large enough for the over water experiments to completely invalidate the relation.

It should be remembered that even though the temperature statistics are obtained at a height where the buoyancy flux is a small fraction of the surface flux, it is the surface flux that is calculated (Z=0) from the temperature statistics at height Z. If the buoyancy flux at the observational height is desired, it must be obtained either by direct measurement or by extrapolating the surface value to the height of observation. The accuracy of this extrapolation depends on the assumptions of the extrapolation model. Figure 8 compares the calculated versus measured "local complete unstable buoyancy flux" for the W data. In this case, the extrapolation is given by the simple linear extrapolation:

$$3)\quad H_Z = H_0(-1.25\ Z/Z_i + 1)$$

where the buoyant flux goes to zero at $Z/Z_i = 0.8$. (The linear decrease of

buoyancy flux with increasing Z/Z_i is implicit in the assumptions of free convective similarity theory.) As expected, the calculated local values of buoyancy flux are less accurate than the surface values, the error becomming worse with increasing Z/Z_i. An important fact to remember is that in the study of most boundary layer processes, eg. by modeling, the surface buoyancy flux, rather than the local buoyancy flux, is a required boundary parameter. The local value by itself is not particularly useful without either a measurement at another height or a knowlege of Z_i in addition to the height of measurement.

The "free convection" approximation to the buoyancy flux provides a good estimate during unstable conditions, when the flux is largest, by the simple measurement of a temperature statistic. This is true even though the temperature measurement is made well above the surface layer, in which the fluxes are constant with height. The effect of ignoring the stability correction to the buoyancy flux estimation can be evaluated by considering the analysis of Figure 8, where the calculated buoyancy flux is given by:

$$4)\ H/RHOc_p = [(\sigma_T/C_1)^3 kgz/T]^{1/2}$$

The difference between the complete unstable and the free convection relations is less than 20% for $-Z/L>0.1$. It departs significantly as neutral conditions are approached, i.e. as the surface is approached for a fixed buoyancy flux and shear stress or as the buoyancy flux decreases or

the shear stress increases at a fixed height during differing conditions. If the stability range is restricted to $-Z/L>0.1$ and the questionable Minnesota data points are excluded, a majority of the estimates are within 25%of exact agreement. Examining the points in Figure 5 that correspond to the values of $Z/Z_i>0.2$ and the stability range $0.1<-Z/L<10.0$, the majority of the largest errors are from the Great Lakes and Puerto Rico experiments: the tower data are well behaved. In the case of the Great Lakes data, the scatter probably is due to inhomogeneity and non-stationarity as the experiment was conducted to study the effect of air mass modification over the Great Lakes during frontal conditions. The Puerto Rico scatter is mainly due to a faulty air temperature sensor and the fact that the data agree to any reasonable extent with the other experiments is due to the dominance of the water vapor contribution to T_v and the buoyancy flux. (Pennell, private communication, 1979)

An important application of this type of technique is the measurement of buoyancy fluxes where the instrumentation packages do not allow the cost or complexity of direct flux measurements or their inference through the flux-gradient relations. An example of such an application, is the Viking Mars Lander Meteorology Instrument where wind speed, wind direction, temperature and pressure were measured at one height. (Chamberlain, et al., 1976) A comparison of fluxes estimated from temperature statistics, using a smaller sample set than optimum and using the free convection approximation, to another indirect method (Sutton, Leovy and Tillman, 1978), indicates

agreement to within 50%. (As the latent heat flux is much smaller than the sensible heat flux, except where CO_2 sublimation is taking place, the buoyancy and sensible heat fluxes are identical in the absence of sublimation.) If the stability dependance and other factors are included, the agreement improves. The lack of better agreement between the two indirect techniques probably is due to the limitations of the current analysis of temperature statistics and the dissimilarities of the data sets analyzed rather than inherent disagreement of the techniques.

The accuracy of the complete calculated/measured buoyancy flux relation, (and implicitly the σ_T/T_* relation) is impressive if it is realized that the data were taken over a 17 year period, by numerous investigators, with differing instrumentation, observational platforms and analysis techniques, over a height range of $0.0<Z/Z_i<0.8$, under stationary and non-stationary conditions as well as over homogeneous and inhomogeneous terrain. Another fact to remember is that the errors in measuring stress and consequently Z/L and T_* may be a major factor contributing to the scatter. Additional experiments with more precise measurements of heat and momentum fluxes and more attention to the other factors will be required to separate the effects of the various parameters and improve the confidence in the basic relation.

Spatial Characteristics of Convective Elements

One of the interesting characteristics of fast temperature measurements in the unstable boundary layer is the periods of almost vanishing temperature fluctuations when the surface layer is super adiabatic or even dramatically auto-convective. Even though the lapse rate can reach almost 100 degrees Celsius per meter in the lowest meter, (Ryan and Carroll, 1970) periods of a half to one minute are encountered during when the fluctuations are on the order of a few hundredths of a degree or less. Parcels with sizes such as indicated by the time scale must originate well above the surface layer and be advected downward into the surface layer by the large scale convection. It is suggested that the large scale convection is responsible for a significant portion of the organization of the smaller elements of the convective boundary layer. Although the demonstration of this hypothesis is beyond this analysis, some insight into the effect of large scale elements on the surface layer can be obtained by considering the uniformity over time and space of temperature during the quiescent intervals.

During stationary conditions, the absoulte temperature within the quiescent intervals repeatedly reaches the same minimum, to within a few hundredths of a degree, when the temperature is devoid of fluctuations greater than the order of 0.01 degrees celsius. If a parcel were advected from a height of several tenths of the inversion height and the height is on the order of a

kilometer or greater, it might be expected to have a uniform potential temperature for one or more of the following reasons:

At it's source height, the vertical and horizontal gradients would be small and slowly varying in time so that parcels advected to the surface sould initially have small fluctuations.

Any fluctuation would be decreased during the downward advection due to mechanical mixing except at the boundaries where entrainment is occurring.

If the statistics of Table 1 are considered, the minimum temperatures of the 4 meter sensors is quite uniform over the array during the 15 minute period, varying by no more than 0.05 degrees. However, the maximum temperature varies by more than 0.25 degrees as the elements are quite small since they originate near the surface. Table 2, at 1719 shortly after the transition to stable at the surface, indicates a reversal of the roles with regard to quiescent temperature. Since the surface has begun to cool radiatively, the potential temperature increases with height and the parcels advected into the surface layer are now warmer than their surroundings during the quiescent interval. During this period, the range of maximum temperatures over the horizontal array is 0.108 degrees while the range of the minimum is 0.268 degrees.

These results are better illustrated in Figure 9 which summarizes these

characteristics for each period. The important characteristic to note is that the variation of the minimum (and equivalently quiescent) temperature is small for the unstable intervals while the variation of the maximum is several times as large. However, when the stability reverses, during the transitional period between 16·07 and 17·19, the roles reverse with the maximum temperature being more consistient in time and space and the minimum less so. (The Minnesota experiment is not unique in illustrating the time variation of the quiescent temperature by itself. However, it's combination of time and space measurements with high accuracy and fast response is unique except for the recent experiment at the Boulder Atmospheric Observatory.)

From these and other observations, (Webb, 1965) it is suggested that if the quiescent temperature in the surface layer has a minimum that repeats to an accuracy of a few hundredths of a degree within a 15 minute interval, and if the fluctuations are on the order of a few hundredths of a degree or less, then the air parcel originated well above the surface layer and it's conservative properties are characteristis of the majority of the well mixed convective boundary layer. To the extent that this is true, then the measurement of conservative properties such as potential temperature, humidity and particulates during these periods can be used to characteize a significant portion of the planetary boundary layer. By combining these with mean measurements, which are characteristic of the surface layer, is may be possible to monitor the evlution of some variables both in and above the surface layer from surface layer measurements.

REFERENCES

Businger, J. A., 1973: Workshop on Micrometeorology, D. Haugen, Ed., American Meteorological Society, 392 pp.

Chamberlain, T. E., H. L. Cole, R. G. Dutton, G. C. Greene and J. E. Tillman, 1976: "Atmospheric measurements on Mars: the Viking Meteorology Experiment." Bull. Amer. Meteor. Soc., Vol. 57, pp. 1094-1104.

Hiester Thomas Ross Parameterization of the unstably stratified planetary boundary layer using aircraft data, thesis, Master of Science, Department of Atmospheric Sciences, University of Washington Seattle Washington, 1977.

Izumi,Y and J. S. Caughey, Minnesota 1973 Atmospheric Boundary Layer Experiment Data Report, Environmental Research Papers, No. 547, Air Force Cambridge Research Laboratories, Hanscomb AFB, Mass., 01731, Unpublished Memorandum, 1976.

Katsaros, K. B., W. T. Liu, J. A. Businger and J. E. Tillman, 1977: "Heat Transport and Thermal Structure in the Interfacial Boundary Layer Measured in an Open Tank of Water in Turbulent Free Convection." J. Fluid Mech. 83, pp 311-335.

Monji, J. "Budgets of turbulent energy and temperature variance in the transitional zone from forced to free convection." thesis, Doctor of Philosophy, University of Washington, Department of Atmospheric Sciences, Seattle, Wa. 98195, 1972.

Munn R. E., 1966: Descriptive Micrometeorology. Academic Press, 245 pp.

Pennell, W. T. and M. A. LeMone, 1974: "An Experimental Study of Turbulence Structure in the Fair-Weather Trade Wind Boundary Layer." J. Atmos. Sci. Vol. 31, pp 1308-1323.

Ryan, J. A. and J. J. Carroll, 1970: "Dust Devil Wind Velocities: Mature State." J. Geop. Res. Vol. 75, pp 531-541.

Shaw, William, J., University of Washington results from the International Turbulence Comparison Experiment, at Deniliquin, New South Wales, Australia. Unpublished memorandum, 1978.

Sutton, J. L., C. B. Leovy and J. E. Tillman, 1978: "Diurnal Variations of the Martian Surface Layer Meteorological zarameters During the First 45 Sols at Two Viking Lander Sites." J. Atmos. Sci. Vol. 35, pp. 2346-2355.

Tillman, J. E., 1972: " The Indirect Determination of Stability, Heat and Momentum Fluxes in the Atmospheric Boundary Layer from Simple Scalar Variables During Dry Unstable Conditions." J. App. Meteor, Vol. 11, pp. 783-792.

Webb, E. K. "Aerial Microclimate." 1965 Meteorological Monograph No. 28, Amer. Met. Soc. Boston, Mass.

Wyngaard J. C., O. R. Cote' and Y. Izumi, 1971: "Local Free Convection and the Budgets of Shear Stress and Heat Flux." J. Atm. Sci., Vol. 28, pp. 1171-1182.

Table 1

Temperature statistics over 15 minutes from the University of Washington and the AFCRL sensors. Temperatures are given in degrees Celsius for the parameters. "T" indicates a UW sensor located on the AFCRL tower at the same height as an AFCRL quartz thermometer mean temperature sensor. The height is given in meters. "C" indicates a UW sensor at the center of the array (Figure 1), located 50 meters to the west of the AFCRL tower, and the height is given in meters. The other designations, "W", "E", and "N" indicate the distance to the west, east and north respectively for the sensor as referred to the center of the array. All of these sensors are located at a height of 4 meters. Sensors are grouped in three groups, with duplicate entries in each group when appropriate for comparison. The first group consists of all sensors on the AFCRL tower and the mean temperature of the UW and AFCRL sensors is identical by definition for this table. For other time periods, these mean temperatures should agree closely if the calibrations are accurate. The next group of sensors are the four at different heights on the mast in the center of the array. The final group include all sensors at the height of 4 meters, irrespective of their location. The sampling interval is 15 minutes over which 45,000 measurements were made for each UW sensor. The MEAN, MIN, MAX, SIGMA and SKEW are the statistics for the given 15 minute period without the removal of any low frequency components or trends. Sensors that are unreliable are

indicated by comments and a thin horizontal line through the data. The skewness is the normalized third moment around the mean. (Tillman, 1972) This period is at the end of a moderately stationary unstable daytime convective time interval.

Table 2

The same functions as Table 1 except at 1719 the surface layer has now become stable.

FIGURE CAPTIONS

Figure (1)

Schematic of array layout for Minnesota field program. Single sensors at a height of 4 meters are indicated by a dot while locations with multiple sensors are indicated by an X. At the array center, sensors are located at heights of 0.5, 1, 2 and 4 meters while on the AFCRL tower, UW sensors are located at heights of 2,4,8,16 and 32 meters, along with AFCRL sensors. The horizontal spacing is 0.64, 2.7, 7.1, 20 and 50 meters.

Figure (2)

σ_T/T_* (where T is replaced by T_v whenever water vapor contributes to the total buoyancy) function of Z/L stratified by experiment for the normalized height range $0.0<Z/Z_i<0.8$. For the AMTEX, BOMEX, GATE, Great Lakes and Puerto Rico experiments, where water vapor is a major factor in determining the buoyancy flux, the virtual temperature is used in place of temperature. The vertical buoyancy flux, $\overline{w'T_v'}$, is used in the computation of L and

$T_{v\star}$.

Figure (3)

$\sigma_T/T_\star$ function of Z/L stratified by Z/Z_i for the normalized height range $0.0<Z/Z_i<1.0$. The characters and their associated ranges are: $0.0<Z/Z_i<0.2$=1, $0.2<Z/Z_i<0.4$=2, $0.4<Z/Z_i<0.6$=3. $0.6<Z/Z_i<0.8$=4, $0.8<Z/Z_i<1.0$=5. The data are characterized by their range of Z/Z_i and the range $0.8<Z/Z_i<1.0$ excluded from 2 , is included to illustrate the increasingly large errors encountered as the inversion is approached· these points are excluded from all subsequent plots.

Figure (4)

$\sigma_T/T_\star$ as a function of Z/L for the AMTEX, BOMEX, GATE, Great Lakes and Puerto Rico experiments for the normalized height range $0.0<Z/Z_i<0.8$. The points indicated by 'V' utilize the virtual temperature while those indicated by 'D' use only dry temperature.

Figure (5)

The ratio of the calculated to measured buoyancy flux at the surface as a function of -Z/L by experiment, computed using the complete unstable relation , 2), for the calculated buoyancy flux. The normalized range of heights are $0.0<Z/Z_i<0.8$ for land and oceanic data from tower and aircraft platforms respectively. The Minnesota data includes both tower and balloon measurements. Where the bouyancy is significantly affected by water vapor, virtual potential temperature replaces temperature both in the direct statistics and in the computation of the parameters. Note the apparent trend of the Minnesota data towards an underestimation of the buoyancy flux for large values of Z/Z_i, due to the balloon measurements.

Figure (6)

The ratio of calculated to measured buoyancy flux as a function of Z/L stratified by Z/Z_i. The points are the same as those of Figure 5 . The

range of normalized inversion height represented by each character is specified in the insert. As no values of inversion height are available for the Kansas, Round Hill and Utah experiments and they were made from towers less than 32 meters high, all data from these experiments are assumed to fall in category 1.

Figure (7)

The ratio of calculated to measured buoyancy flux as a function of the *actual measured* buoyancy flux for the height range $0.0<Z/Z_i<0.8$.

Figure (8)

The ratio of complete unstable calculated/measured buoyancy flux as a function of Z/Z_i. The data are clasified as surface values, dots, and local values, crosses. Local of buoyancy flux are obtained by extrapolating the surface values values (determined from local values of temperature statistics) to the height of measurement using the linear extrapolation.

given by 3). Tower measurements are excluded from this plot as Z/Z_i is generally unknown and the local and surface values are essentially identical.

Figure (9)

The ratio of calculated/measured buoyancy flux as a function of Z/L stratified as a function of Z/Z_i. The calculated buoyancy flux uses the "free convection" approximation, given by 4). Exact agreement for the complete unstable relationship is indicated by the thin lower curve. Data include the height range $0.0<Z/Z_i<0.8$.

Figure(10)

Statistical properties of temperature over time and the array. The top curve illustrates the Obukhov stability paramerer for each 15 minute run, going from unstable at the beginning to stable during the last period. The stability values are derived from the profiles of wind and temperature, via the flux- gradient relations. The second curve gives the mean wind speed at

4 meters during the same inteval. The group of three curves in the lower figure all present data from the 15 minute statistics over the horizontal array at the 4 meter height. The upper of the three curves illustrates the behavoir of the mean temperature over the array during each 15 minute period. For each time, there is a minimum and a maximum temperature displayed along with a standard deviation. The standard deviation is indicated by the heavy bar which is PM one standard deviation around the mean. In this case, the mean is the average of all mean temperatures and the standard deviation, Min and Max refer to statistics of the mean temperature of all sensors during the given 15 minute period. The reason for the equivalence of the data for the mean temperature at 15:07 is that the sensors were defined to have the same mean temperature at this time for cross calibration with AFCRL. The minimum and maximum temperature plots are constructed in the same manner as that of the mean, ie. from the minimum and maximum temperatures at each location during the 15 minute interval.

DATE	START TIME	LENGTH	# SAMPLES
9/28/72	1719 0	900 sec	45000

LOCATION	AFCRL	MEAN	MIN	MAX	SIGMA	SKEW
T 32.0	22.75	22.803	22.661	22.922	0.0449	0.0276
~~T 16.0~~	~~22.85~~	~~22.965~~	~~22.686~~	~~23.115~~	~~0.0614~~	~~-0.3903~~
T 8.0	22.84	22.891	22.457	23.104	0.0952	-0.5297
T 4.0	22.86	22.911	22.417	23.179	0.1178	-0.4054
T 2.0	22.76	22.776	22.278	23.082	0.1116	-0.1997
C 4.0		22.876	22.421	23.107	0.0960	-0.4411
C 2.0		22.855	22.359	23.134	0.1179	-0.6390
~~C 1.0~~	~~22.81~~	~~23.128~~	~~22.640~~	~~23.443~~	~~0.1239~~	~~-0.3594~~
C 0.5	22.89	23.157	22.603	23.575	0.1641	-0.1739
T 4.0		22.911	22.417	23.179	0.1178	-0.4054
C 4.0		22.876	22.421	23.107	0.0960	-0.4411
W 0.6		22.881	22.470	23.115	0.0960	-0.4239
E 0.6		22.862	22.413	23.100	0.0935	-0.3380
W 2.7		22.882	22.408	23.112	0.0947	-0.3650
N 2.7		22.898	22.410	23.155	0.0950	-0.4736
E 2.7		22.896	22.481	23.126	0.0955	-0.4478
~~W 7.0~~		~~22.893~~	~~22.511~~	~~23.150~~	~~0.1030~~	~~-0.1636~~
E 7.0		22.895	22.535	23.129	0.0914	-0.4468
E 20.0		22.954	22.676	23.167	0.0684	-0.3564
N 50.0		22.929	22.486	23.208	0.1031	-0.2830

Table 2

DATE	START TIME	LENGTH	# SAMPLES
9/28/72	1507 0	900 sec	45000

Location	AFCRL Mean	UW Mean	Min	Max	Sigma	Skew
T 32.0	22.79	22.792	22.420	23.815	0.2520	0.7879
~~T 16.0~~	~~23.08~~	~~22.396~~	~~21.941~~	~~23.644~~	~~0.3039~~	~~0.6062~~
T 8.0	23.19	23.192	22.609	24.743	0.3943	0.7999
T 4.0	23.47	23.471	22.738	25.144	0.4629	0.7174
T 2.0	23.66	23.661	22.650	25.754	0.5614	0.5978
C 4.0		23.472	22.704	25.006	0.4287	0.4923
C 2.0		23.662	22.772	25.098	0.4125	0.2709
~~C 1.0~~		~~24.509~~	~~23.630~~	~~25.631~~	~~0.3179~~	~~0.1899~~
C 0.5		24.522	23.334	26.049	0.3916	0.1895
T 4.0		23.471	22.738	25.144	0.4629	0.7174
C 4.0		23.472	22.704	25.006	0.4287	0.4923
W 0.6		23.472	22.702	24.981	0.4216	0.4802
E 0.6		23.472	22.706	25.040	0.4254	0.5011
W 2.7		23.472	22.710	24.953	0.4170	0.4854
N 2.7		23.472	22.732	25.136	0.4401	0.5808
E 2.7		23.472	22.713	25.102	0.4336	0.5411
~~W 7.0~~		~~23.472~~	~~22.206~~	~~25.169~~	~~0.4304~~	~~0.5101~~
E 7.0		23.472	22.726	24.909	0.4460	0.5565
E 20.0		23.472	22.728	25.225	0.4295	0.4789
N 50.0		23.472	22.760	25.111	0.4302	0.4390

Table 1

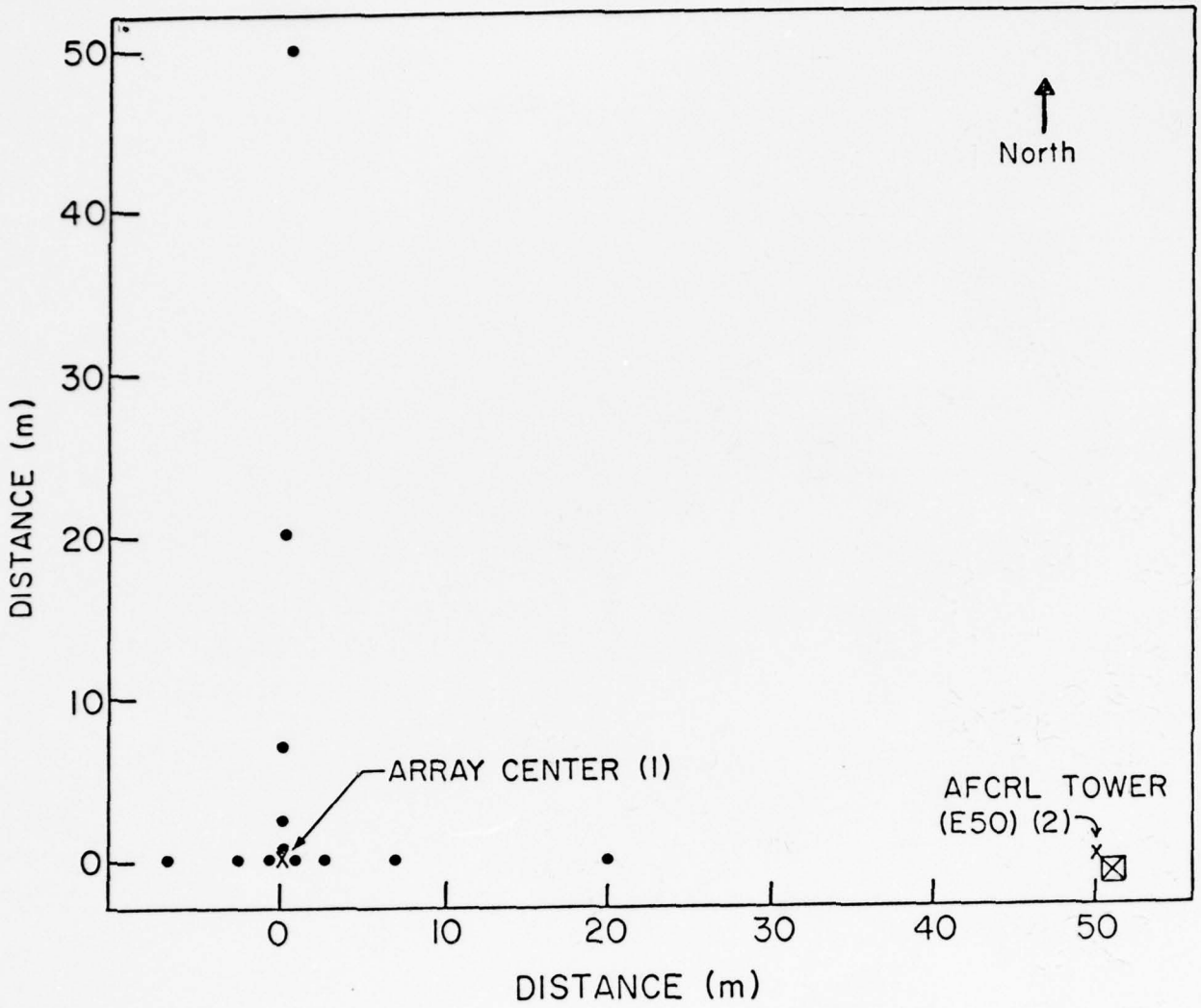

LOCATIONS OF TEMPERATURE SENSORS FOR MINNESOTA FIELD PROGRAM

Figure 1

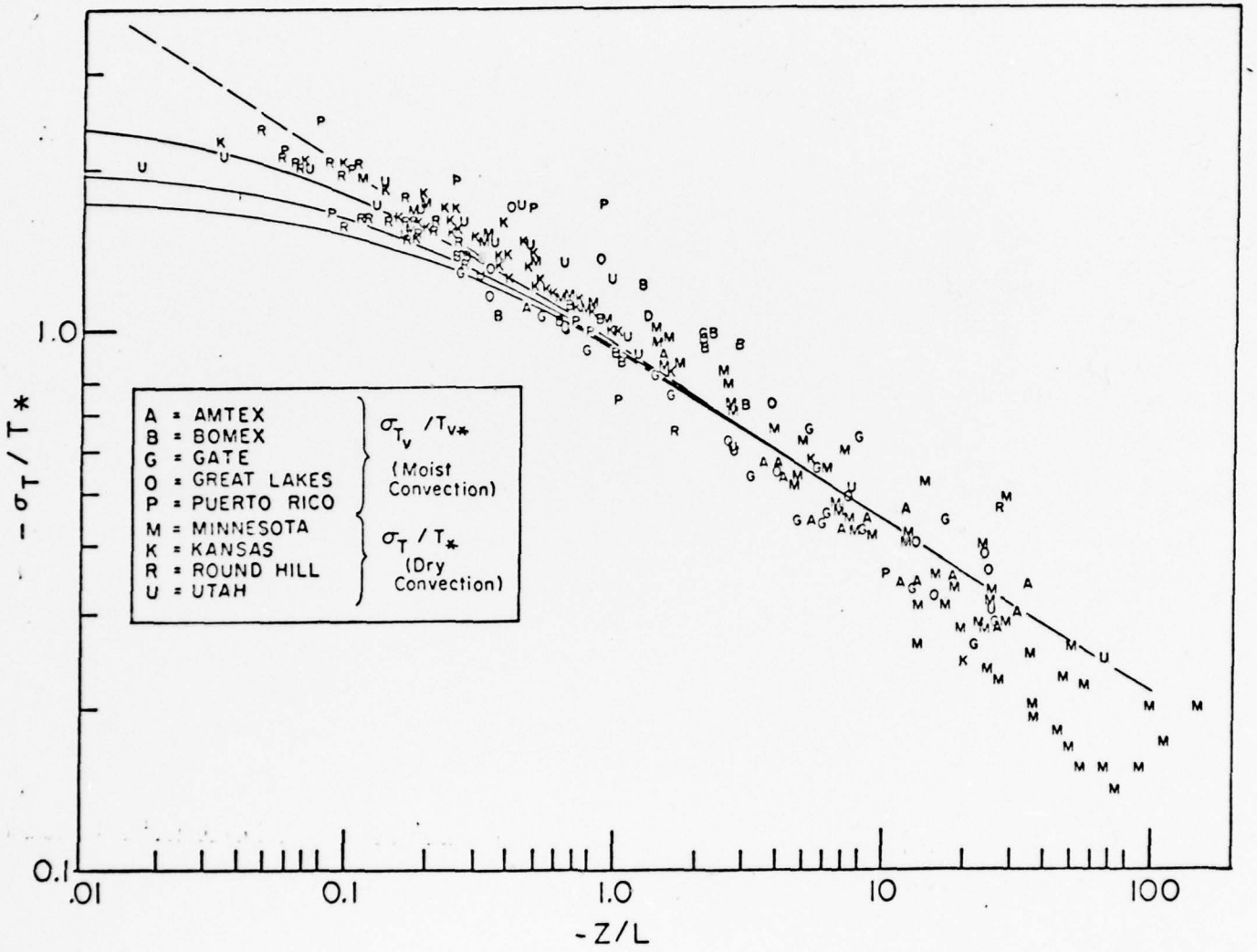
A = AMTEX
B = BOMEX
G = GATE
O = GREAT LAKES
P = PUERTO RICO
M = MINNESOTA
K = KANSAS
R = ROUND HILL
U = UTAH
σ_{T_v} / T_{v*} (Moist Convection)
σ_T / T_* (Dry Convection)
$-\sigma_T / T_*$
1.0
0.1
.01
0.1
1.0
10
100
-Z/L

Figure 2

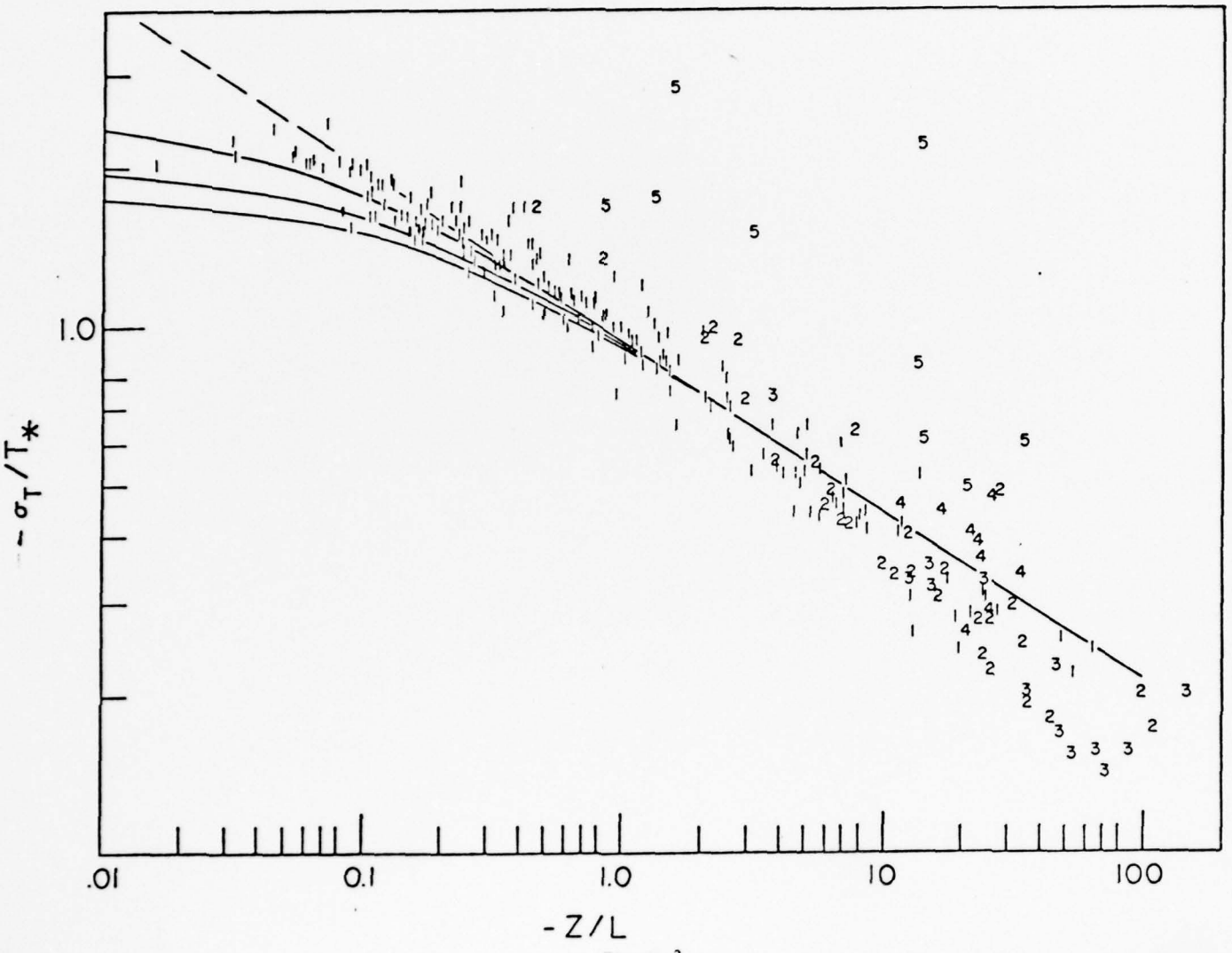

Figure 3

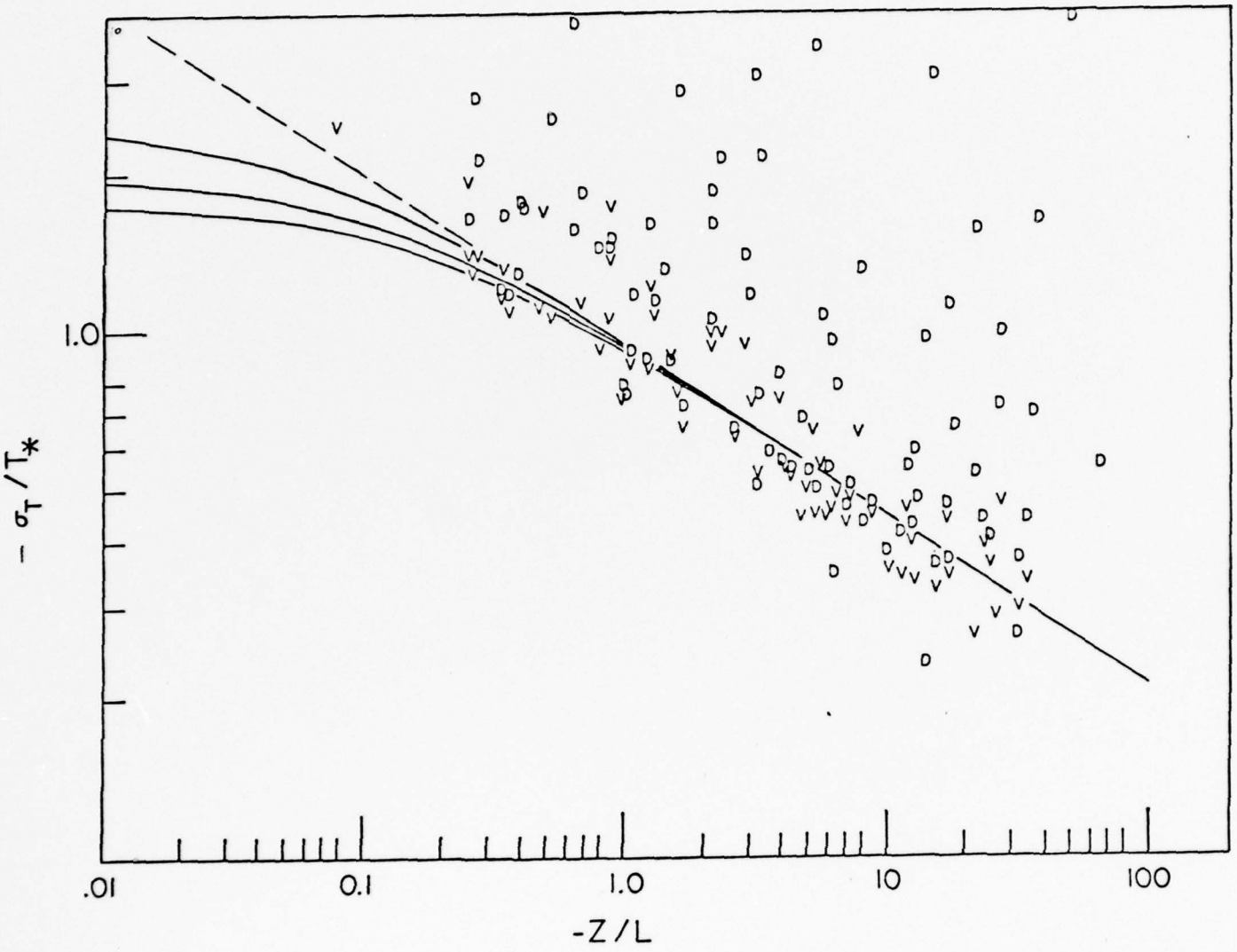

Figure 4

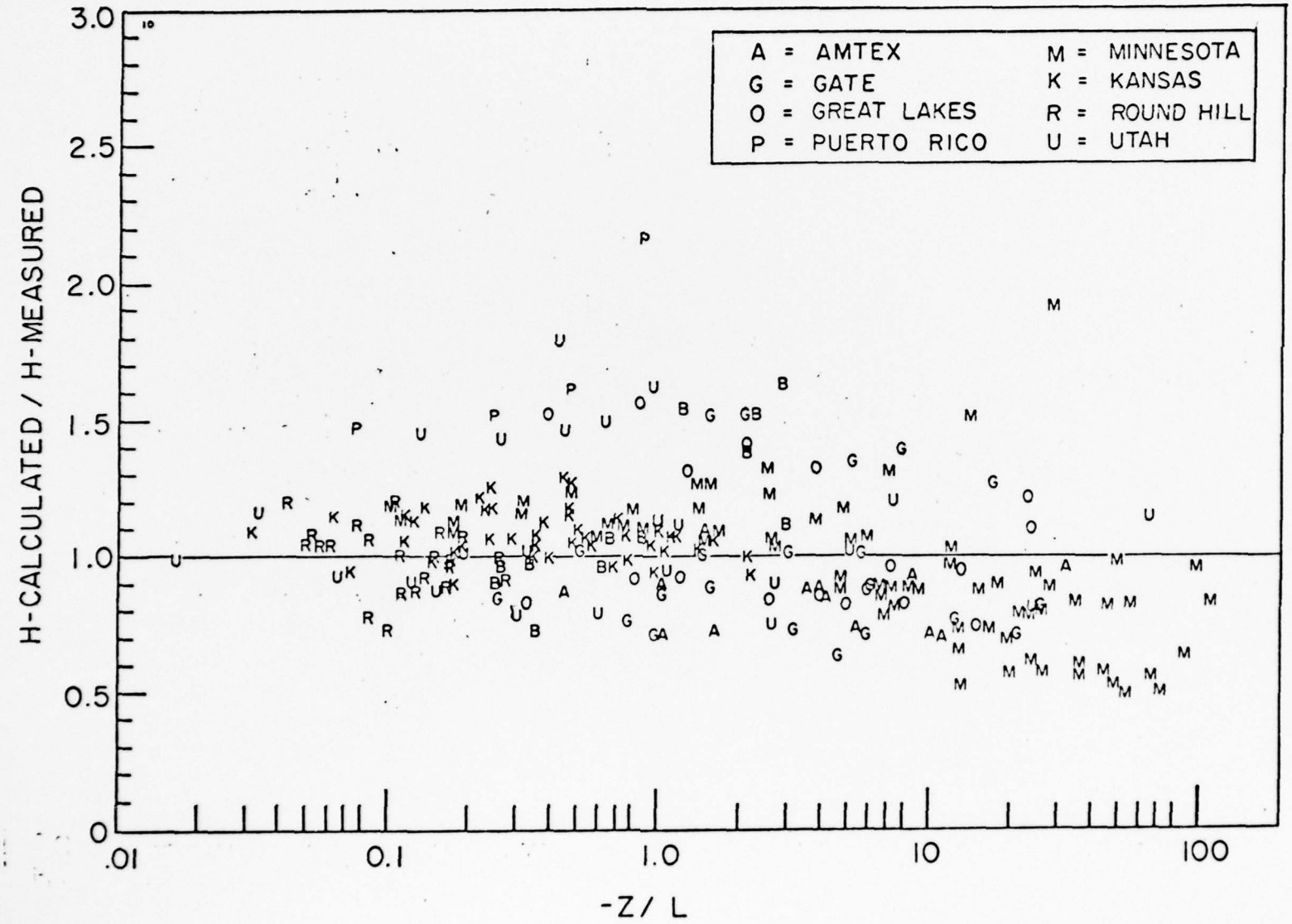
A = AMTEX
G = GATE
O = GREAT LAKES
P = PUERTO RICO
M = MINNESOTA
K = KANSAS
R = ROUND HILL
U = UTAH
H-CALCULATED / H-MEASURED
-Z/ L
3.0
2.5
2.0
1.5
1.0
0.5
0
.01
0.1
1.0
10
100

Figure 5

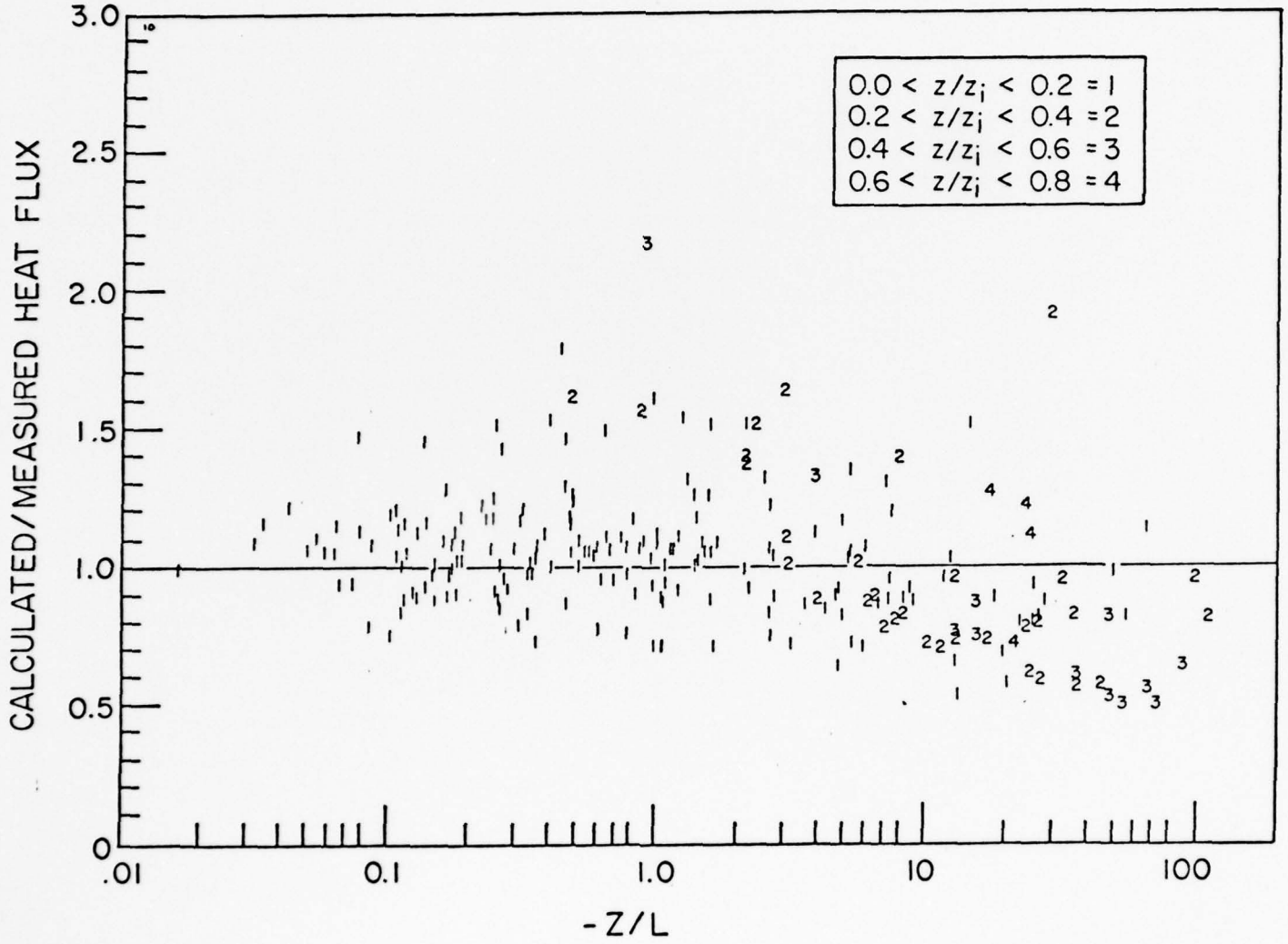
0.0 < z/z_i < 0.2 = 1
0.2 < z/z_i < 0.4 = 2
0.4 < z/z_i < 0.6 = 3
0.6 < z/z_i < 0.8 = 4
CALCULATED/MEASURED HEAT FLUX
3.0
2.5
2.0
1.5
1.0
0.5
0
.01
0.1
1.0
10
100
-Z/L

Figure 6

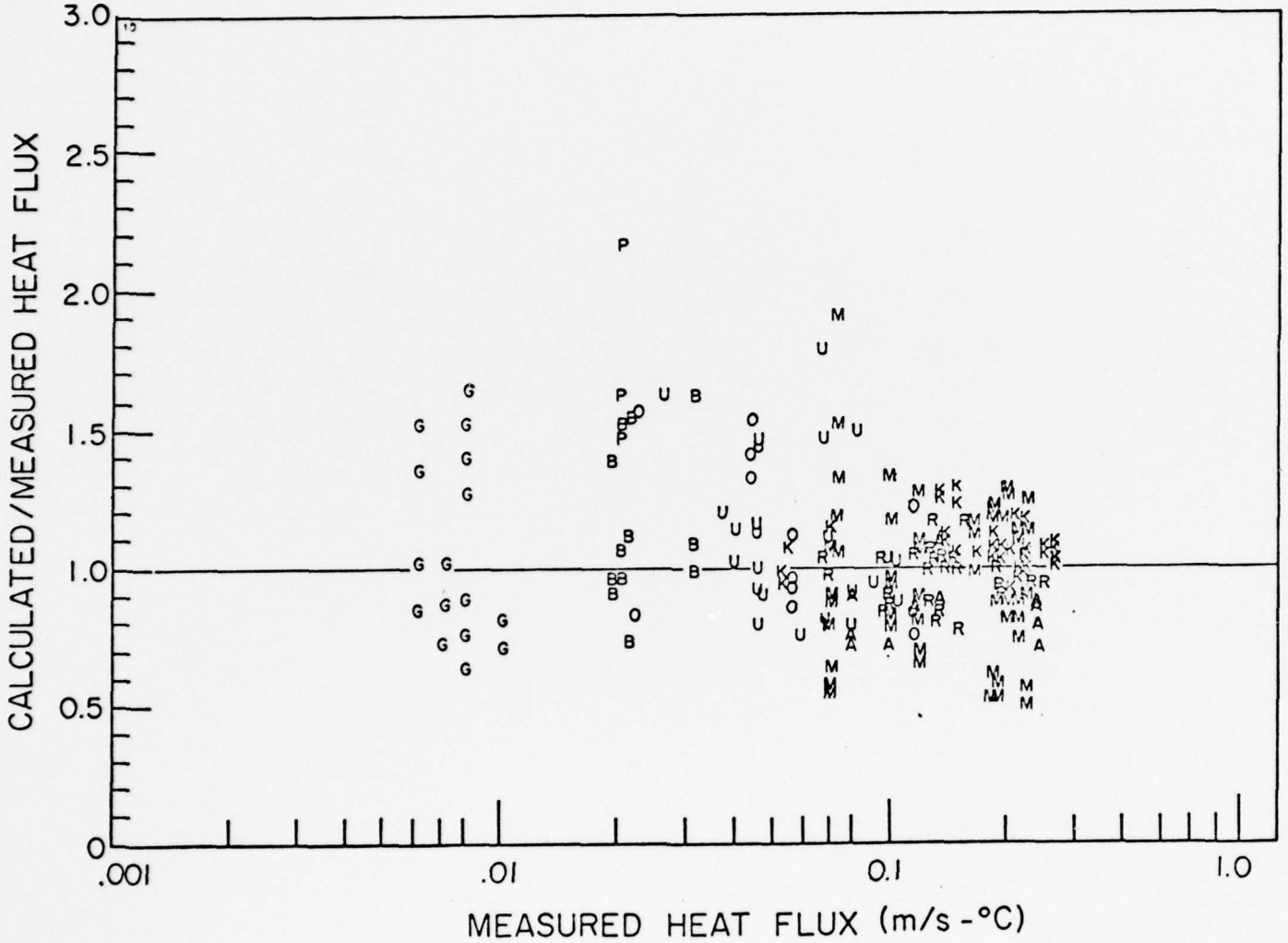
CALCULATED/MEASURED HEAT FLUX
3.0
2.5
2.0
1.5
1.0
0.5
0
.001
.01
0.1
1.0
MEASURED HEAT FLUX (m/s -°C)

Figure 7

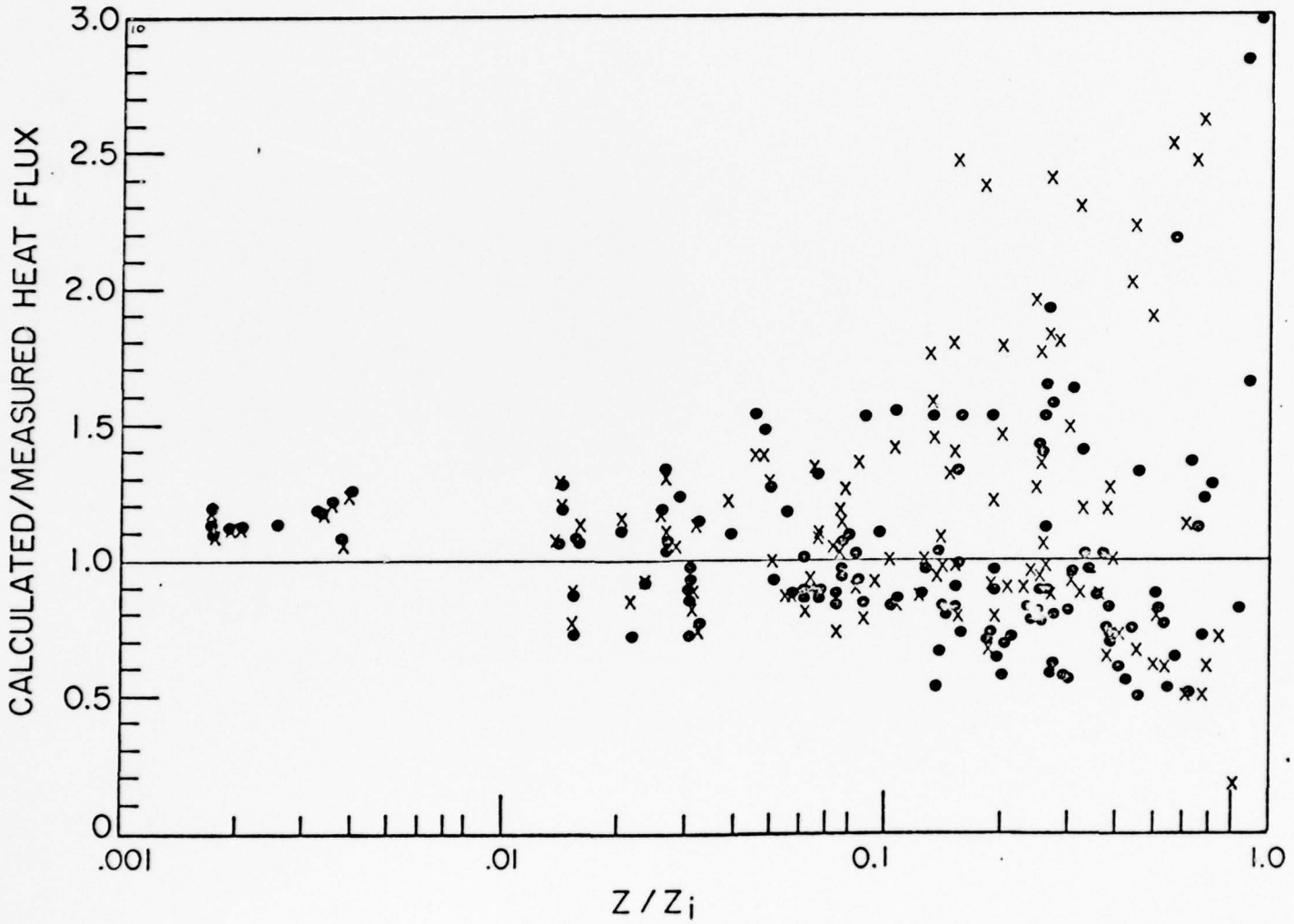
CALCULATED/MEASURED HEAT FLUX
3.0
2.5
2.0
1.5
1.0
0.5
0
.001
.01
0.1
1.0
Z / Zi

Figure 8

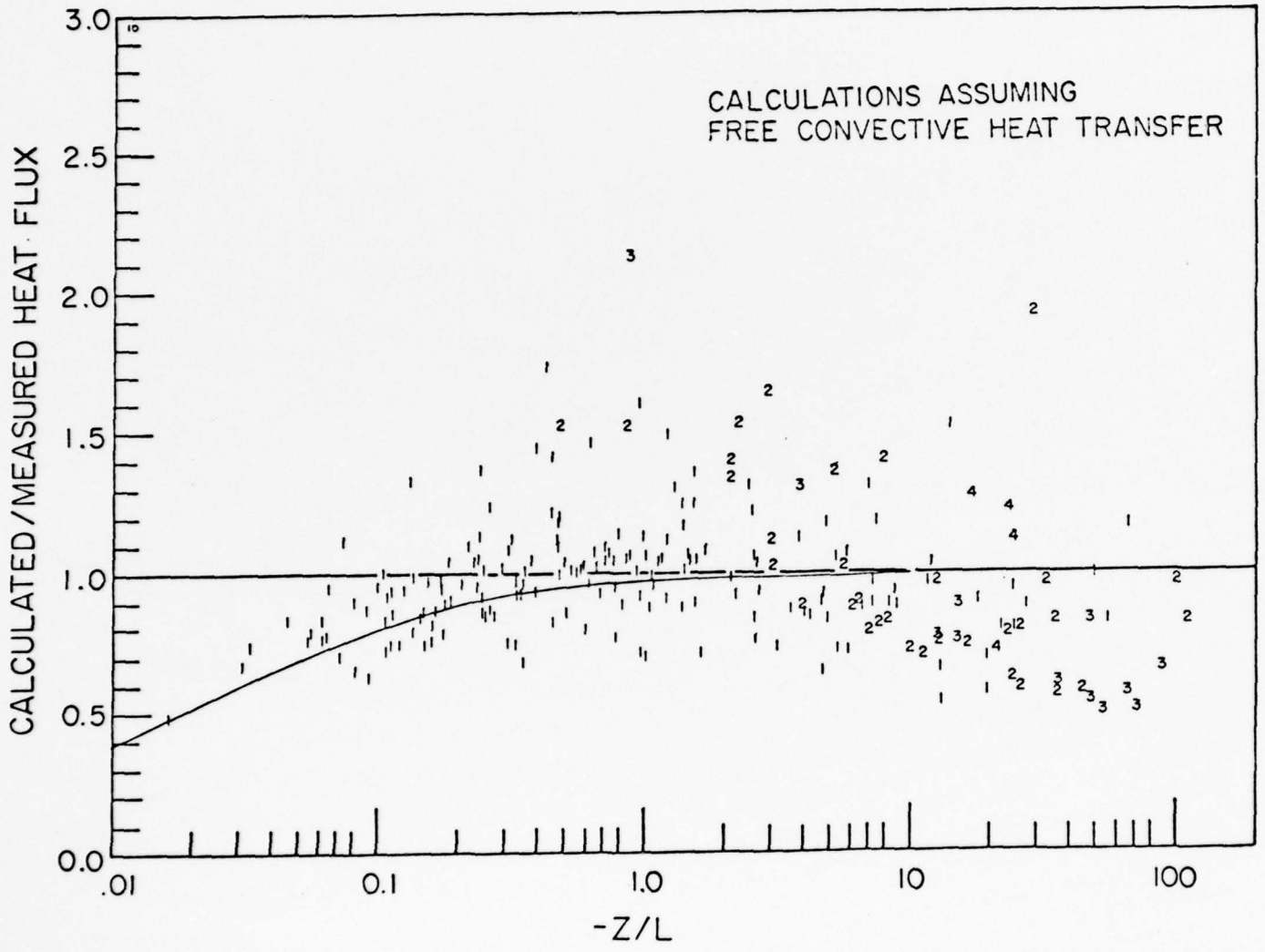
CALCULATIONS ASSUMING
FREE CONVECTIVE HEAT TRANSFER
CALCULATED/MEASURED HEAT FLUX
3.0
2.5
2.0
1.5
1.0
0.5
0.0
.01
0.1
1.0
10
100
-Z/L

Figure 9

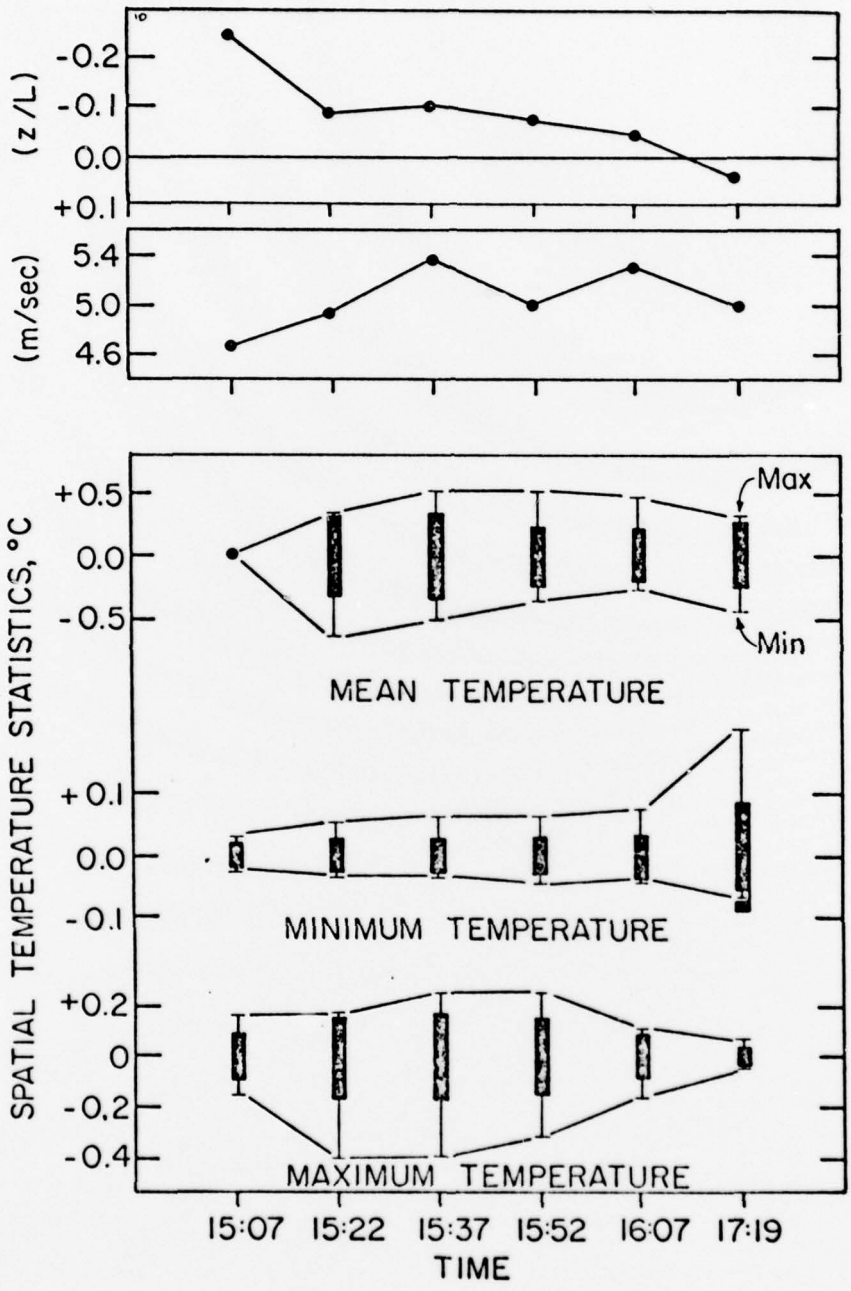
(z/L)
-0.2
-0.1
0.0
+0.1
(m/sec)
5.4
5.0
4.6
SPATIAL TEMPERATURE STATISTICS, °C
+0.5
0.0
-0.5
Max
Min
MEAN TEMPERATURE
+0.1
0.0
-0.1
MINIMUM TEMPERATURE
+0.2
0
-0.2
-0.4
MAXIMUM TEMPERATURE
15:07
15:22
15:37
15:52
16:07
17:19
TIME

Figure 10

ACKNOWLEDGEMENT:

The grant provided some support to the following students:

Ken Richmond
Tom Heister
Siri Jodha Singh Khalsa
Jim Wilczak

No degrees were granted.

Portions of this report are being prepared for publication.